Biochimica et Biophysica Acta 1848 (2015) 2385–2393

Contents lists available at ScienceDirect

Biochimica et Biophysica Acta

journal homepage: www.elsevier.com/locate/bbamem

Topological analysis of the Na^+/H^+ exchanger

Yongsheng Liu, Arghya Basu, Xiuju Li, Larry Fliegel *

Department of Biochemistry, University of Alberta, Edmonton, AB T6G 2H7, Canada

ARTICLE INFO

Article history:
Received 17 February 2015
Received in revised form 20 July 2015
Accepted 21 July 2015
Available online 26 July 2015

Keywords:
Na^+/H^+ exchanger
Membrane protein
Topology model
pH regulation

ABSTRACT

The mammalian Na^+/H^+ exchanger isoform 1 (NHE1) is a ubiquitously expressed integral membrane protein present in mammalian cells. It is made up of a hydrophobic 500 amino acid membrane domain that transports and removes protons from within cells, and a regulatory intracellular cytosolic domain made of approximately 315 amino acids. Determining the structure of NHE1 is critical for both an understanding of the Na^+/H^+ exchange mechanism of transport, and in the design of new improved inhibitors for use in treatment of several diseases in which it is involved. Differing models of the NHE1 protein have been proposed. The first model suggested by two groups proposes that amino acids 1–500 form a 12 transmembrane segment spanning region in which amino acids 1–127 form two transmembrane segments, and amino acids 315–411 form a single transmembrane segment with membrane associated segments. A second model based on the structure of the *Escherichia coli* Na^+/H^+ exchanger protein proposes an overall similar topology, but suggests amino acids 1–127 are removed as a signal sequence and are not present in the mature protein. It also suggests a different topology of amino acids 315–411 to form three transmembrane segments. We used cysteine scanning accessibility and examination of glycosylation of the mature protein to characterize the NHE1 protein. Our results demonstrate that the model of NHE1 is correct which suggests that amino acids 1–127 form two transmembrane segments that remain connected to the mature protein, and the segment between amino acids 315–411 is one transmembrane segment.

1. Introduction

The Na^+/H^+ exchanger (NHE) is a membrane transport protein ubiquitously present in living organisms. In mammals, its primary function is to protect cells from excess intracellular acid, which it achieves by catalyzing the electroneutral removal of a single intracellular H^+ in exchange for one extracellular Na^+. The ubiquitous isoform one (NHE1), was the first isoform discovered in 1989 [1,2]. Ten isoforms of NHE are currently known to exist (NHE1–10) with different tissue expression, cellular localization and physiological roles. Some types are mainly present on intracellular organelles (NHE6–9) while others NHE1–5, are mainly plasma membrane proteins. NHE1 is made up of 815 amino acid residues separated into two domains — an N-terminal transmembrane (TM) domain where ion transport is catalyzed and a C-terminal cytosolic domain that regulates the ion transport activity [3].

The major physiological role of NHE1 is regulation of intracellular pH but it is also involved in cell differentiation, cell proliferation, cell volume regulation, cytoskeletal organization and cell migration. In transformed cells, alkalinization mediated by NHE1 plays also an important role in the development of the transformed phenotype and this is prevented when NHE1 is inhibited [4,5]. NHE1 also plays a clear role in mammalian development. Mice with a NHE1 deletion have decreased postnatal growth and increased mortality, ataxia and epileptic seizures [6] and we have recently demonstrated that homozygous expression of a defective NHE1 gene in humans results in disease, with a phenotype including hearing loss and cerebellar ataxia [7].

The structure of the *Escherichia coli* Na^+/H^+ exchanger NhaA [8] and that of NapA from *Thermus thermophilus* has been elucidated [9]. Briefly, the crystal structure of NhaA [8] contained two groups of 6 transmembrane (TM) segments each had two three TM bundles. TMIV and TMX1 make a novel fold with extended non-helical regions that crossed and were thought to contain various charged residues important for ion binding and transport. That protein was in an acid locked state and not active however the structure of NapA was determined in an active state with significant differences from NhaA. A two domain, rocking bundle, alternating access model of sodium proton antiport was hypothesized [9] though elements of this model have been disputed [10]. The structure of another Na^+/H^+ exchanger, the archaeal Na^+/H^+ antiporter NhaP1, has been determined at 7Å resolution and it varies from NhaA with 13 membrane spanning TM segments instead of 12, but the 6 helix bundle structure is conserved and similar to that of NhaA [11].

While significant progress has been made describing the prokaryotic Na^+/H^+ exchanger NhaA structure and on some other primitive types,

Abbreviations: BCECF-AM, 2′,7′-bis(2-carboxyethyl)-5(6) carboxyfluorescein-acetoxymethyl ester; CHO, Chinese hamster ovary; HA, hemagglutinin; NHE1, Na^+/H^+ exchanger type 1 isoform; pHi, intracellular pH; WT, wild type.

* Corresponding author.
E-mail address: lfliegel@ualberta.ca (L. Fliegel).

http://dx.doi.org/10.1016/j.bbamem.2015.07.011
0005-2736/

only limited progress has been made on deciphering the structure of the mammalian isoforms of the protein. Mammalian Na^+/H^+ exchangers have little homology to NhaA and a 1:1 stoichiometry, in contrast to the 2:1 stoichiometry of NhaA. The NHE1 isoform is the only mammalian type with significant progress made in direct examination of its structure. While the entire protein is resistant to large scale overexpression and crystallization, we have been able to examine the structure of TM segments by NMR [12–18]. These studies have revealed interesting characteristics of the TM segments that are similar to some segments of NhaA. However, they cannot give a complete picture of the structure of the protein without a better understanding of the overall topology of the protein.

Wakabayashi et al. [19] used cysteine scanning accessibility experiments to make an initial analysis of the topology of NHE1. They suggested a 12 TM model based on the accessibility of the residues tested with the N- and C-terminus in the cytoplasm. They proposed two intracellular loops, between TMs IV–V (amino acids 176–190) and VIII–XI (316–338), which contained amino acids that were accessible extracellularly but were suggested to be intracellular and part of re-entrant loops (Fig. 1A, B). Amino acids 341–362 formed TM segment IX, and extracellular loop 5 that was thought to be associated with the membrane. An alternate 3D model of NHE1 was later proposed based on the structure of NhaA as a template [20]. This model also contained 12 TM helices but had several notable differences. It did not include the first two helices of the model of the Wakabayashi model (1–125), which were thought to be removed by cleavage (Fig. 1A). TMIX (339–359) was assigned as two short helices and a re-entrant segment between TMIX-X is reassigned as TMIX (374–398) (Fig. 1C). This rearrangement of the re-entrant loop placed EL5 (360–410), which had numerous extracellularly accessible residues [19], on the inside of the membrane. They suggested that this loop could be near the pore of the protein, accounting for this accessibility. The last three TMs (411–505) are the same in both models (Fig. 1). More recently Nygaard et al. [21] proposed a model of NHE1 that was based on the NhaA model and on the work of Wakabayashi et al. [19]. The model of Nygaard et al. [21] has also proposed a 12 transmembrane structure of NHE1. The overall two dimensional configuration of this model is similar to that of the Wakabayashi model with the main differences in the membrane segments being the beginning and end of some of the helices. Most of the beginnings and ends of the transmembrane segments were very similar (TM's I–VIII, and X–XII), varying by 2–5 amino acids while TMIX was amino acids 339–359 and 333–353 in these two models, respectively [19,21] (the models were recently reviewed by [22]). Nygaard et al. attempted to verify one part of their model using electron paramagnetic resonance, but their final model suggested that the charged side chain of D172 is critical to NHE1 function and it has been shown that mutation of this residue to N or Q did not impair NHE1 function [23]. Clearly a greater refinement of existing models of NHE1 is necessary and more direct characterization of the structure of NHE1 is necessary. The controversy in the area has continued [24,25].

In the present study, we examined the accessibility of numerous amino acid residues of the mature NHE1 protein, to distinguish between these three models. We studied the regions that are more controversial, the N-terminal amino acids 1–127 and the segment containing amino acids 315–411. Further, we used immunoprecipitation of the mature surface protein and an analysis of the N-linked glycosylation of the protein to study the N-terminal transmembrane segments. The results are consistent with amino acid residues 1–127 forming two transmembrane segments that remain connected to the mature protein, and the segment between amino acid residues 315–411 forming one transmembrane segment as proposed by Wakabayashi et al.'s [19] model.

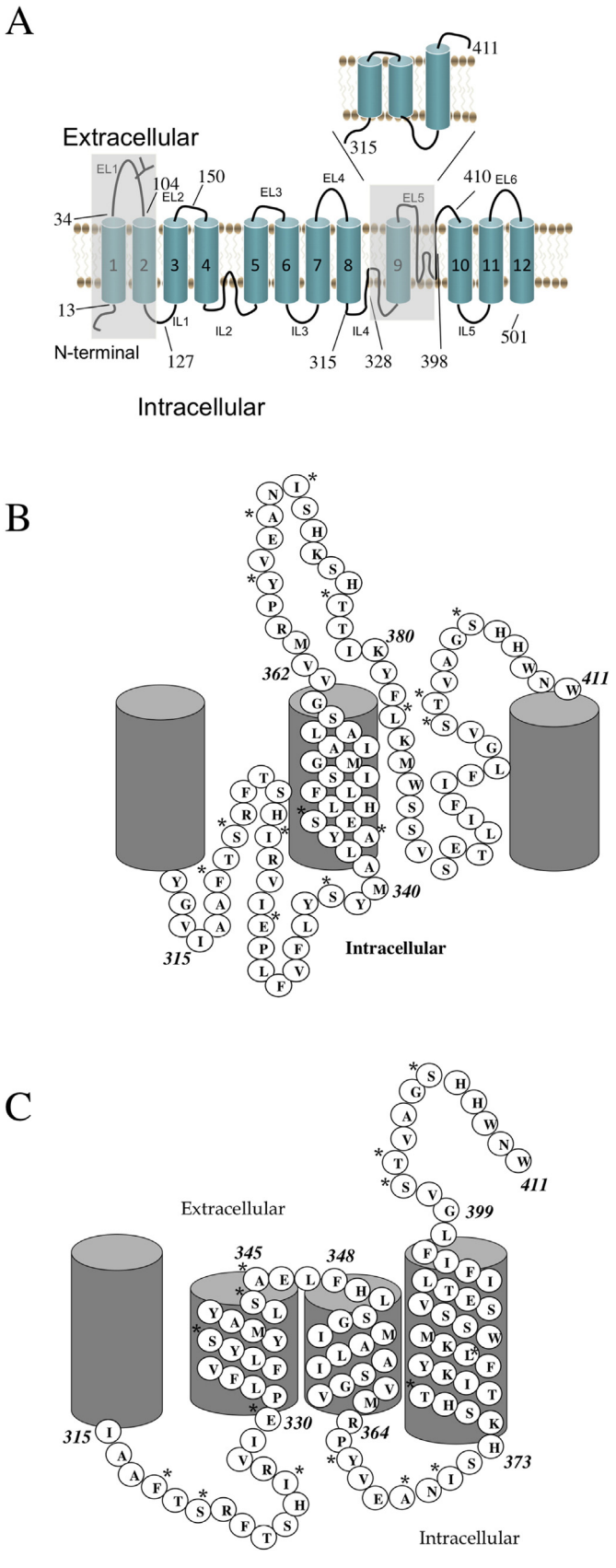

Fig. 1.

Fig. 1. Models of topology of the NHE1 protein. A, Schematic diagram of transmembrane domain of NHE1 protein. Transmembrane segments 1–12 are illustrated together as suggested by Wakabayashi et al. [19,21] (model #1). Shaded areas are regions in dispute in model #2 [20]. Transmembrane segments 1–2 were suggested to be deleted in model #2. An alternate topology of amino acid residues 315–411 is illustrated above from model #2. B and C show detailed alternative topologies of amino acid residues 315–411 models #1 and #2, respectively. EL, extracellular loop; IL, intracellular loop. * indicates amino acid mutated to Cys in the present study.

2. Materials and methods

2.1. Materials

2′,7'-Bis(2-carboxyethyl)-5(6) carboxyfluorescein acetoxymethyl ester (BCECF-AM) was from Molecular Probes, Inc. (Eugene, OR). Streptavidin agarose and streptolysin O were purchased from Sigma, (St. Louis, MO, USA), Sulfo-NHS-SS-biotin was obtained from Pierce Chemical Company (Rockford IL, USA) and synthetic DNA was purchased from IDT (Coraiveille, IA, USA). Immobilized streptavidin was from Sigma-Aldrich (St Louis MO, USA). Geneticin antibiotic was from American Bioanalytical (Natick MA, USA). O-Glycosidase and PNGaseF were from New England Biolabs Inc. Cell culture MEM alpha modification medium was purchased from Thermo Fisher Scientific Hyclone (Logan UT, USA). pH measurements used 2′,7′-bis (2-carboxyethyl)-5(6) carboxyfluorescein-acetoxymethyl ester purchased from Molecular probes, Inc. (Eugene OR, USA). PWO DNA polymerase was from Roche Applied Science (Roche Molecular Biochemicals, Mannheim, Germany). For transfection, Lipofectamine 2000 reagent was from Invitrogen Life Technologies (Carlsbad CA, USA). Other chemicals that were used were of analytical grade and were from Fisher Scientific (Ottawa, ON, Canada), Sigma (St. Louis, MO, USA) or BDH (Toronto, ON, Canada). The plasmid pYN4+ has been described earlier [26] and contains the human NHE1 protein with a C-terminal HA (hemagglutinin) tag. We have earlier shown the cysteineless NHE1 (cNHE1) is fully functional [7].

2.2. Site-directed mutagenesis

Site-directed mutagenesis was on cNHE1 as described earlier [18]. Mutations were designed to create or delete a restriction enzyme site. DNA sequencing confirmed the fidelity of DNA amplification and mutations. Table 1 summarizes the mutations made.

2.3. Cell culture and stable transfection

To characterize the activity of the Na^+/H^+ exchanger we used mutant Chinese hamster ovarian cells that do not express endogenous NHE1 (AP-1 cells) [1]. Stably transfected cells were made using LIPOFECTAMINE 2000 Reagent (Invitrogen Life Technologies, Carlsbad, CA, USA) as described earlier [18]. The NHE1 expression plasmid (pYN4+), contains a neomycin resistance gene for selection of stably transfected cells using geneticin (G418). Stable cell lines for experiments were regularly re-established from frozen stocks at passage numbers between 5–11. Results are typical of at least two stable cell lines of each type of mutant.

2.4. Cell surface expression

Targeting of the NHE1 protein to the cell surface was measured as described earlier using sulfo-NHS-SS-biotin labeling [27]. Briefly, the cell surface was labeled with sulfo-NHS-SS-biotin and cells were solubilized. The cell surface NHE1 protein was removed from solubilized proteins with immobilized streptavidin resin. We used SDS-PAGE and western blotting to examine equal amounts of unbound and total protein using anti-HA (NHE1-tag) antibodies. The image densities on the western blots were estimated using Image J 1.35 software (National Institutes of Health, Bethesda, MD, USA). It was not possible to efficiently and reproducibly elute proteins bound to immobilized streptavidin resin. The amount of NHE1 on the plasma membrane was estimated by comparing both the upper and lower HA-immunoreactive species.

2.5. Accessibility of residues

The accessibility of residues of NHE1 was determined based on procedures we have used earlier [13]. Stable cell lines with mutations in NHE1 were grown to confluence and washed with phosphate buffer saline (PBS). They were then treated +/− 10 mM MTSET for 20 min at 37 °C in a buffer consisting of 135 mM NaCl, 5 mM KCl, 1.8 mM $CaCl_2$, 1.0 mM $MgSO_4$, 5.5 mM glucose and 10 mM HEPES, pH 7.3 (normal buffer). Cells were washed three times with PBS and then 2 ml of a lysis buffer was added, consisting of 25 mM Tris HCl, pH 7.4, 150 mM NaCl, 1 mM EDTA, 1% NP-40, 5% glycerol and 37.5 μM ALLN and a protease inhibitor cocktail [28]. Cells were scraped off and sonicated two times for 15 s. The solution was spun at 35,000 rpm (100,000 ×g) for 1 h and the supernatant was collected. HA-tagged NHE1 protein was immunoprecipitated from the supernatant. For immunoprecipitation we used the Pierce Crosslink IP kit in which the primary antibody was crosslinked to Protein A/G agarose beads. This enabled immunoprecipitation without contamination from the primary antibody. The primary antibody used for immunoprecipitation was a commercially obtained rabbit polyclonal against the HA tag (Santa Cruz, sc-805). After immunoprecipitation, the sample was divided into two. One sample was used to quantify the total NHE1 protein via western blotting. To the second sample IRDye800-maleimide (LI-COR) was added (final concentration 0.2 mM) which would react with any unblocked sulfhydryls of the introduced cysteine. Samples were separated by SDS-PAGE and we examined the protein, which reacted with the IRDye800-maleimide using a LI-COR system. Calculations were, MTSET accessibility = 100 − %(Fluorescence in the presence MTSET / Fluorescence in absence of MTSET). Readings were corrected for the amount of NHE1 which was immunoprecipitated by Western blotting for NHE1 with a monoclonal antibody against the HA tag.

In some experiments, cells were permeabilized with streptolysin O prior to determination of accessibility of intracellular loops. Mutant cell lines (S8C, F318C, S320C, I326C, S338C, A345C) were prepared as described above. Briefly, cells were washed with PBSCM (PBS plus 0.1 mM $CaCl_2$ and 1 mM $MgCl_2$) two times, followed by washing the cells with cold incubation buffer (25 mM Hepes; 115 mM potassium acetate; 2.5 mM $MgCl_2$; 1 mM dithiothreitol; pH 7.4). Cells were incubated with (or without) 350 units/ml SLO in 2 ml of incubation buffer for 15 min on ice. Cells were washed with warm incubation buffer (37° C30 min) and then with PBSCM. They were treated +/− MTSET (10 mM) in normal buffer for 20 min at 37°C. Then washed 3 times with PBS. Cells were then harvested and examined for NHE1 accessibility as above.

Table 1
Oligonucleotides used for site-directed mutagenesis of cNHE1. Mutated nucleotides are lower case, restriction sites created are bold, (–) denotes site removed.

A

Mutation	Oligonucleotide sequence	Site
S8C	GGTCTGGCATCTgcGG**cttaag**TCCACATCGGATC	AflII
S44C	GCCCAACTGCC**tGtACa**ATTCGAAGCTCAG	BsrGI
T97C	GGCATCGACTACtgtCACG**TcCGgA**CCCCCTTC	BspEI
T101C	CACACGTGCGCtgCCCCTTCGAaATCTCCCTCTG	–BglII
F318C	CGGGGTCATCGCA**GCaTgC**ACCTCCCGATTTAC	SphI
S320C	CGCAGCCTTCAC**CTgCaG**ATTTACCTCCCAC	PstI
I326C	CGATTTACCTCCCA**CtgCaG**GGTCATCGAGCCG	PstI
E330C	CACATCCGGGT**CATatg**cCCGCTCTTCGTC	NdeI
S338C	GTCTTCCTCTACtGCTACATGGCCTACTTGT **CtGCaG**AGCTCTTCCAC	PstI
S344C	GCCTACTTGTgtGCCGAaCTCTTCCACCTG	–SacI
A345C	GCCTACTTGTCAtgCGAaCTCTTCCACCTG	–SacI
Y366C	GATGCGCCCCTgtGTGGAGGCC**AAtATt**TCCCACAAGTC	SspI
A369C	CTATGTGGAGtgC**AAtATt**TCCCACAAGTC	SspI
I371C	GTGGAGGCCAA**CtgCag**CCACAAGTCCCAC	PstI
T377C	CACAAGTCCCAC**tgtACa**ATCAAATACTTC	BsrGI
L383C	CACCATCA**AATAtT**TCtgtAAGATGTGGAGC	SspI
S401C	CTTCCTCGGCGTC**tgtACa**GTGGCCGGCTC	BsrGI
T402C	GGCGTCTCCtgcGTGGCC**GGaTCC**CACCAC	BamHI
S406C	CCTCGGCGTC**agtACt**GTGGCCGGCtgCCACCACTGG	ScaI

2.6. SDS-PAGE and immunoblotting

Expression of NHE1 was confirmed by immunoblotting using antibodies against the HA tag on the NHE1 C-terminus. Samples were run on 10% SDS-PAGE gels and were electrotransferred to nitrocellulose membranes for incubation with anti-HA monoclonal antibody. The secondary antibody used for signal detection was peroxidase-conjugated goat anti-mouse antibody (Bio/Can, Mississauga, Canada). Reactive protein was detected on X-ray film using the Amersham enhanced chemiluminescence western blotting and detection system.

2.7. Intracellular pH measurement

BCECF was used to measure NHE1 activity and to quantify intracellular pH (pH*i*) recovery after an acute acid load as described earlier [18]. Cells were grown to ≈90% confluence on coverslips and fluorescence was measured using a PTI Deltascan spectrofluorometer with the parameters described earlier. Briefly, acute acidosis was induced by ammonium chloride prepulse, 50 mM × 3 min addition followed by withdrawal. The first 20 s of recovery from acidification and was measured as ΔpH/s. Calibration of intracellular pH fluorescence was done for each sample as described earlier [18]. Results are shown as the mean ± S.E. of at least 6 experiments and statistical significance was determined using the Wilcoxon Signed-Rank test. Variations in the level of surface targeting and protein expression were used to correct for activity of the protein as described earlier [15,29].

2.8. Characterization of glycosylation

A series of experiments were carried out to characterize NHE1 glycosylation and to determine if NHE1 protein was glycosylated at N75 of the first extracellular loop, and if NHE1 containing glycosylation at N75 was present at the cell surface. AP1 cells were transiently transfected with wild type HA-tagged NHE1 cDNA [7]. Proteins present at the cell surface were labeled with sulfo-NHS-SS-biotin as described earlier [18] and immobilized streptavidin resin was used to remove cell surface labeled protein. Briefly, cells were grown to confluence in 100 mm plates and were rinsed sequentially with 4 °C PBS and borate buffer [154 mM NaCl, 7.2 mM KCl, 1.8 mM $CaCl_2$, and 10 mM boric acid (pH 9.0)]. The cells were then incubated for 30 min at 4 °C in borate buffer, containing sulfo-NHS-SS-biotin (0.5 mg/ml). Cells were washed with quenching buffer [192 mM glycine and 25 mM Tris (pH 8.3)] and then harvested with 500 μl of ice cold IPB [1% (v/v) IGEPAL CA-630, 0.5% (w/v) deoxycholic acid, 150 mM NaCl, 5 mM EDTA, and 10 mM Tris–HCl (pH 7.5)], containing complete protease inhibitor and solubilized for 20 min on ice. Tubes containing cell lysates were centrifuged for 20 min at 13,000 *g* and 4 °C. The supernatant was collected in a fresh tube. Depending on the experiment, the supernatant was divided into two equal parts and both sets were incubated separately with 50 μl of streptavidin agarose resin for 16 h at 4 °C with gentle rotation. The supernatant was collected after centrifugation for 2 min at 8000 *g*. The resin from one of the two sets, which now has bound biotinylated proteins, was treated with 500 U of PNGase F (NEB) [1 μl from stock], 1× G7 (provided with PNGase F) reaction buffer and 1% NP-40 at 37 °C for 4 h. Resin in the other tube was treated similarly with only 1× G7 reaction buffer and 1% NP-40. Tubes were vortexed every 10–15 min for proper enzyme action. After 4 h resin from both tubes were treated with SDS-PAGE sample buffer at 65 °C for 10 min. Samples were run on 10% acrylamide SDS-PAGE gel and transferred to PVDF membrane. Immunoblotting was with anti-HA monoclonal antibody as described earlier [27].

Another series of experiments used NHE1-HA cDNA that had N75 mutated to D as described earlier, which would prevent N-linked glycosylation [30]. Cells were transiently transfected with one of the two NHE1 cDNA's and then the size of the NHE1 protein was examined by immunoblotting in either whole cell lysates or in intact cells.

3. Results

3.1. Alternative topologies

Fig. 1 outlines the alternative topologies of the NHE1 protein. Model #1 is based on the topologies of Wakabayashi et al. and Nygaard et al. [19,21]. Given the minor differences in the ends of the transmembrane segments of these two models [22], one representative two-dimensional model was used referred two as model 1. Here amino acid residues 1–127 remain as an integral part of the intact full-length protein and amino acid residues 315–411 have two membrane associated regions and one transmembrane segment. In model #2, the first two transmembrane segments were proposed to be cleaved and removed as a signal sequence [20] while an alternative topology was proposed for amino acid residues 315–411 (Fig. 1B, C). To test these differing hypotheses we made a series of mutants of the cysteineless NHE1 protein inserting single cysteine residues in the two areas of contention (Table 1). Nineteen mutations were successfully made in the cNHE1 protein and stable cell lines were successfully made expressing each of these mutant copies of NHE1. The mutations were in the proposed intracellular N-terminus (S8C), in the first extracellular loop (S44C, T97C, T101C) and a series of fifteen mutations in a contentious region from residues 315–411 (Fig. 1B,C). Five other mutations were attempted (I128C, V334C, M340C, M363C and T378C) but for reasons that are presently unclear, we were not able to obtain either successful mutations or stable cell lines expressing these mutations.

3.2. Characterization of mutants

Initially we characterized the expression, activity and cell surface targeting of all mutants to ensure that an active and properly folded protein was obtained. The results are shown in Fig. 2. A comparison of the levels of expression of the various mutant proteins is shown in Fig. 2A. Most of the mutants expressed NHE1 at levels similar to that of the control, +/− 20%. A few, A345C, T377C, L383C and S406C were up to 50% lower in expression levels but still had easily identifiable and quantifiable protein.

Fig. 2B shows that most of the mutants had levels of surface processing similar to that of the control, cysteineless NHE1. The Y366C and I371C mutants were up to 12% lower in targeting compared to control, though still had appreciable levels of protein targeted to the cell surface.

We then compared the activity of the mutants to that of the cNHE1 protein (Fig. 2C). Most of the mutant proteins retained over or near 40% of the value of the control. A few, T101C, E330C, A345C, and L383C were less than 25% of the control level. The E330C and L383C mutant proteins were under 16% of the control level activity, and were excluded from further experiments on accessibility. When correcting for the amount of protein and the surface targeting it was apparent that the same mutants, T101C, E330C, A345C, and L383C had defective protein activity that was due to an effect on the protein itself and not due to defective targeting or expression levels.

3.3. Accessibility studies

To gain novel insights into the topology of the NHE1 protein and to compare and contrast the two existing models of the protein we examined the surface accessibility of the mutant amino acid residues that were present in functional NHE1 proteins. The results are shown in Fig. 3. Fig. 3A shows one typical result and Fig. 3B a summary of 3–5 experiments. NHE1 mutant proteins with cysteine residues at amino acid residue positions, S8, S44, F318, S320, I326, S338, S344, A345, I371 and S406 were not accessible to MTSET blockage of reaction with IRDye800-maleimide. NHE1 mutant proteins with cysteine residues at amino acid positions T97, T101, Y366, A369, T377, S401 and T402 were susceptible to MTSET blockage of reaction with IRDye800-maleimide. As the

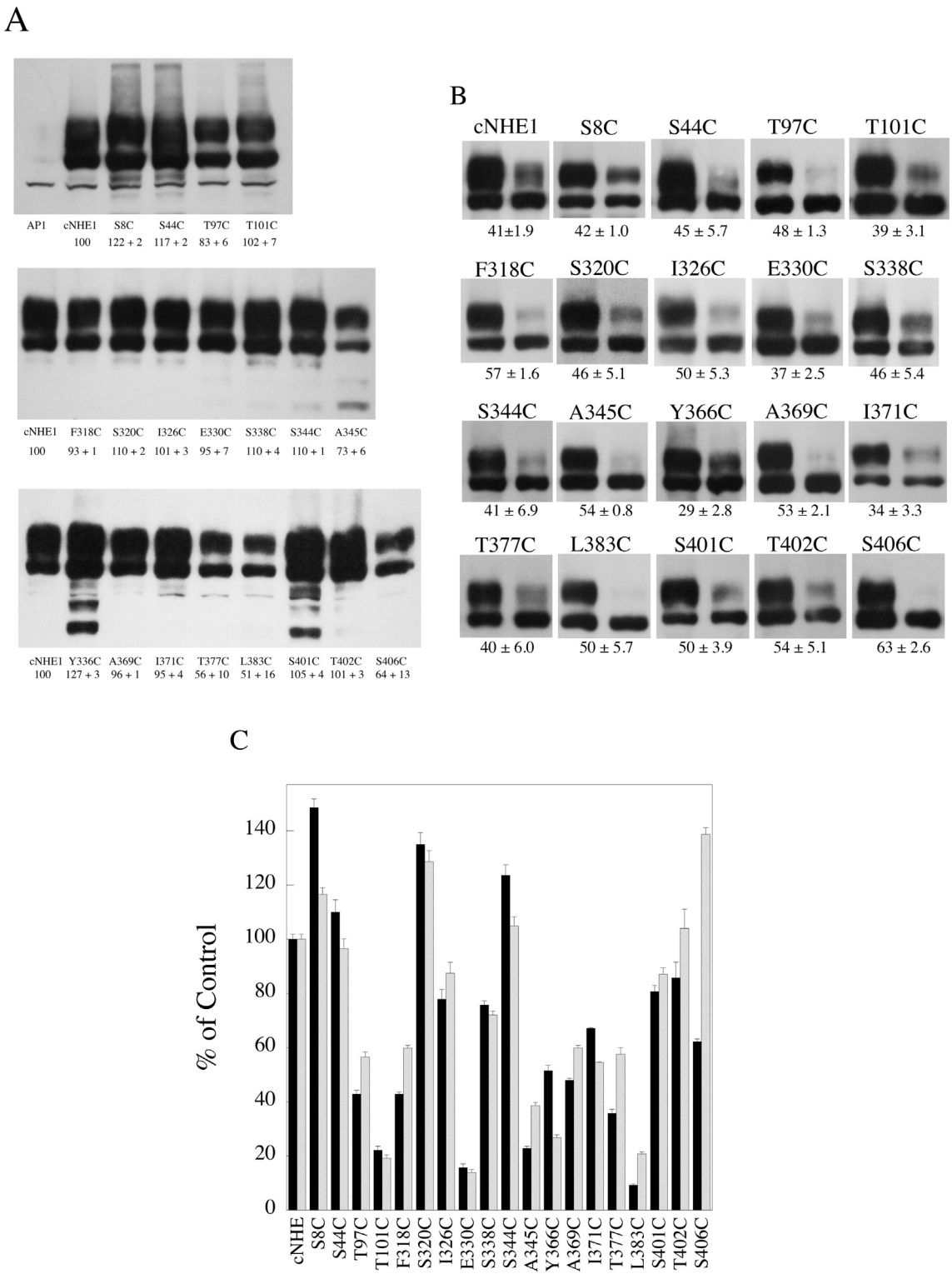

Fig. 2. Characterization of Na^+/H^+ exchanger mutants expression, targeting and activity. A, Western blot of cell lysates of stable cell lines expressing full length Na^+/H^+ exchanger mutants or control NHE1 protein using anti HA-antibody. Mutations are indicated. Equal amounts of cell lysate were loaded in each lane. Numbers below each lane indicate the amount of Na^+/H^+ exchanger protein relative to wild type Na^+/H^+ exchanger. Mean values ($n > 3$–4) were obtained from both the 110 and 95-kDa bands. AP-1 refers to AP-1 cells not transfected with NHE1. Wt, refers to cells stably expressing wild type cysteineless NHE1 protein. B, Surface localization of NHE1 in AP-1 cells expressing control or NHE1 mutant proteins. Equal amounts of total cell lysate (left lane) and unbound intracellular lysate (right lane) were examined using Western blotting with anti-HA antibody to identify the NHE1 protein. cNHE1 is from a cell line stably expressing cysteineless NHE1 protein. The percent of the total NHE1 protein found on the cell plasma membrane is indicated for each mutant. Results are the mean ± the S.E. n = at least 3 determinations. C, Summary of the rate of recovery after an acute acid load of AP-1 cells transfected with wild type NHE1 and Na^+/H^+ exchanger mutants. The mean control activity of cells stably transfected with NHE1 was .014 Δ pH/s, and this value was set to 100%. Other activities are a percent of those of cNHE. Values are the mean ± SE of 6–10 determinations. Results are shown for mean activity of both uncorrected (black) and normalized for surface processing and expression levels (cross hatch).

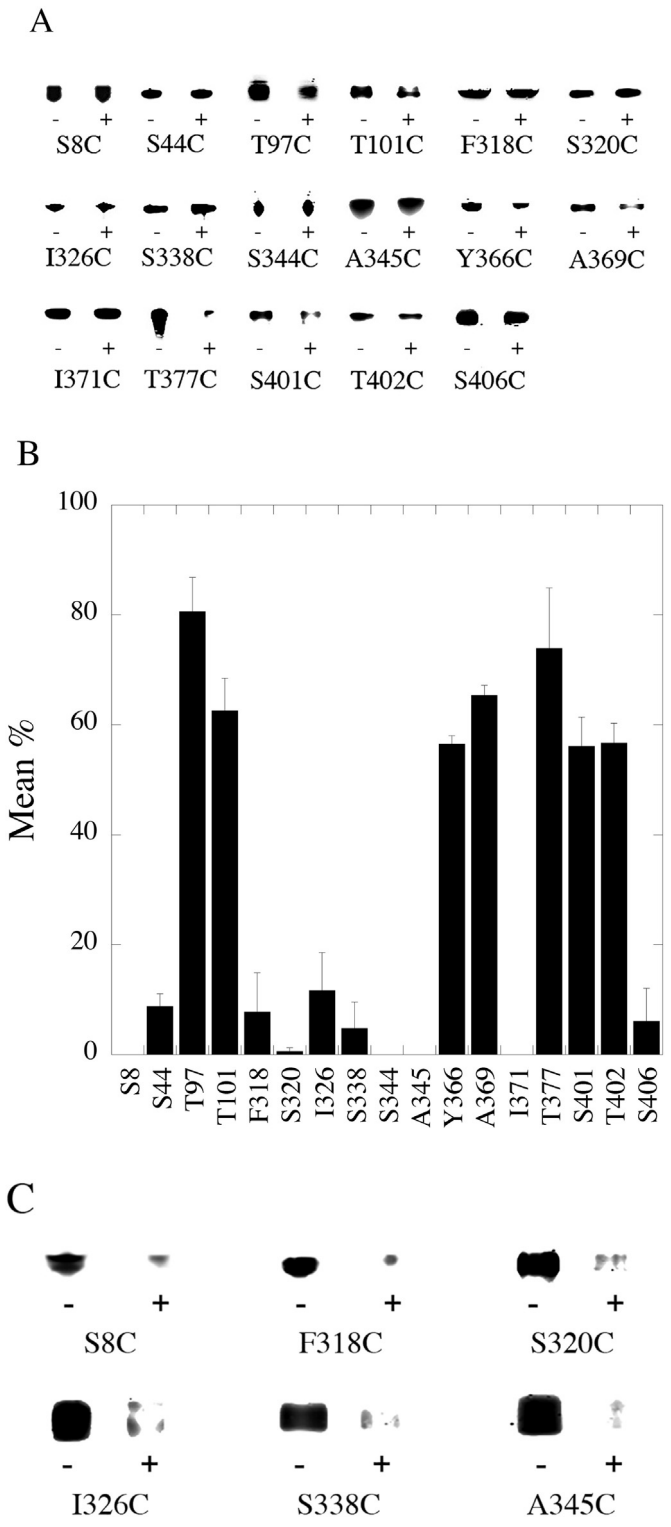

Fig. 3. The accessibility of cysteine residues of NHE1 mutants to reactivity with MTSET was measured as described in the "Materials and methods". A, Illustrates examples of MTSET blocking of reactivity with IRDye800-maleimide. Prior reaction with MTSET blocks the reactivity with IRDye800-maleimide when the residue is accessible. + indicates reacted with MTSET prior to reaction with IRDye800-maleimide. B, Summary of the accessibility of various NHE1 mutant proteins. Results are the mean ± SE of at 3–5 experiments. C, Effect of cell permeabilization on accessibility of putative intracellular amino acids of NHE1. Cells (S8C, F318C, S320C, I326C, S338C, A345C) were treated with or without streptolysin O as described in the Materials and methods. They were then tested for accessibility as described above + indicates reacted with MTSET prior to reaction with IRDye800-maleimide. Results are typical of at least 3 experiments.

experiment was done in intact live cells and MTSET is impermeable to the plasma membrane, this indicated that these residues were accessible to the extracellular surface.

To confirm that residues S8, F318, S320, I326, S338 and A345 of the NHE1 protein were intracellularly located we permeabilized cells with streptolysin O and examined the accessibility of these residues to MTSET (Fig. 3C). Treatment with streptolysin O, allowed MTSET blockage of the reaction with IRDye800-maleimide. This suggested that these residues were accessible on the intracellular surface.

3.4. Study of N-linked carbohydrates and extracellular loop 1

Cysteine scanning accessibility experiments of the first extracellular loop suggest that the protein that is present on the extracellular surface contains this segment. However, an argument could be made that this represents a subfraction, perhaps a minority, of the entire NHE1 protein. To counter this argument, we did experiments in which we examined the status of cell surface NHE1 protein. We determined if NHE1 at the cell surface contained glycosylated NHE1 protein by labeling cell surface proteins with sulfo-NHS-SS-biotin. Immobilized streptavidin was used to pull down labeled surface proteins. Cell surface proteins were treated with PNGaseF, which catalyzes removal of N-linked oligosaccharides from glycoproteins. The results are shown in Fig. 4A. Treatment with PNGaseF caused an increase in mobility of the NHE1 protein confirming that NHE1 on the cell surface contains N-linked oligosaccharides.

Based on current topology models of NHE1 [19,20], the consensus sequence of N-linked glycosylation, and a previous report [31], N75 is the only site for N-linked carbohydrate addition. We confirmed that N75 of the first extracellular loop, is used for glycosylation. AP1 cells were transfected with either wild type NHE1 protein or with NHE1 protein that had an N75 to D mutation. Western blot analysis of total proteins of cell lysates showed that the NHE1 protein with a N75D mutation was of reduced molecular size compared to the wild type Fig. 4B.

We also examined if the N75D containing NHE1 protein was present at the cell surface (Fig. 4C). Cell surface proteins were labeled with sulfo-NHS-SS-biotin and immobilized streptavidin was used to pull down labeled proteins. Both wild type and N75D proteins were present on the cell surface and the apparent molecular weight of the N75D protein was again reduced, in comparison to the wild type NHE1 protein.

4. Discussion

4.1. NHE1 physiological significance

The topology of the NHE1 protein is of great interest both from a purely scientific point of view and from an applied standpoint. Scientifically, the mechanism of Na^+/H^+ exchange is of great interest to a wide audience. While significant progress has been made in the structure and function of prokaryotic Na^+/H^+ exchangers [8] much less has been made in the analysis of mammalian NHE's which has little homology to bacterial Na^+/H^+ antiporters and a different stoichiometry (reviewed in [3]). Na^+/H^+ exchange represents a fundamental and critical cellular process being important in cell growth, human development and differentiation [32]. It thus is of great fundamental interest to science.

Aside from a fundamental science point of view, mammalian NHE1 is an important putative target in several diseases. It is important in ischemic heart disease, heart hypertrophy and plays a critical facilitative role in some types of cancer [5,33–35]. NHE1 inhibitors have been developed to provide cardioprotection from heart disease unfortunately these have not been very successful, possibly due to poor administration protocols that lead to non specific effects of the inhibitor [36]. While a myriad of NHE1 inhibitors has been developed [37], a fundamental knowledge about their specific site of interaction with the protein is unclear [38] and though TMVI of NHE1

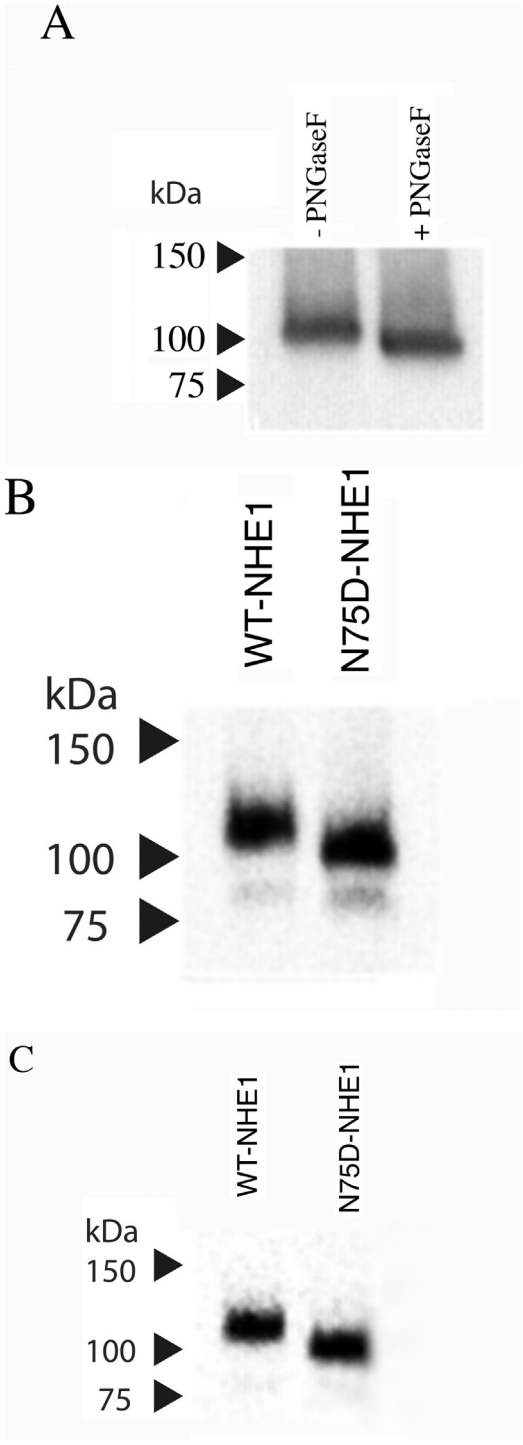

Fig. 4. Characterization of N-linked glycosylation site of NHE1. A, Cells were transfected with HA-tagged NHE1 containing plasmid and cell surface proteins were labeled by biotinylation. Surface accessible proteins were precipitated with immobilized streptavidin and then treated with PNGAseF as described in the "Materials and methods". Western blot analysis was with anti-HA antibody. B, Cells were transfected with HA-tagged NHE1 protein or with NHE1 protein with the N75D mutation. Whole cell lysates were probed by Western blot analysis as described in "A". C, Cells were transfected with HA-tagged Wt NHE1 containing plasmid or plasmid with the N75D mutation. Cell surface proteins were obtained as described in "A". Western blot analysis was with anti-HA antibody.

has been implicated as being involved in NHE1 inhibitor sensitivity [39], clearly a greater understanding of the basic structure of NHE1 is desirable, to lead to the design of new and improved inhibitors.

4.2. Evidence towards alternative topology models

As noted above, two fundamentally different types of model of NHE1 have been put forth. One was by the group of Wakabayashi [19] which used cysteine scanning accessibility experiments and was later refined by Nygaard et al. [21] (model #1). A second and different model (model #2) was by the group of Landau et al. which modeled NHE1 after the structure of NhaA [20]. The fundamental differences between these two models are illustrated in Fig. 1. Briefly, the model of Landau et al. suggested that transmembrane segments encompassing the first 125 amino acid residues were deleted from the full-length protein (Fig. 1A) and also proposed a different topology for amino acid residues 315–411 (Fig. 1B,C). The predicted topology of residues 126–314 and residues 412–500 is quite similar in the model of Landau, Nygaard and Wakabayashi as recently reviewed [22].

Our experiments with cell surface accessibility were on two regions of the protein. The proposed first two transmembrane segments are residues 1–125 and the region from residue 315 to residue 411. Model #2 [20] suggested that these two transmembrane segments could be cleaved and removed in the mature NHE1 protein. This is in contrast with model #1. Wakabayashi [19] also directly demonstrated that several amino acids on extracellular loop 1 were extracellular according to cysteine accessibility studies. Our results support the inclusion of the first two transmembrane segments as part of the whole intact NHE1 protein in the topology proposed by model #1 by Wakabayashi et al. [19] and Nygaard et al. [21]. Firstly, we found that proteins containing amino acid residues that we mutated in this region were fully expressed similar to the wild type NHE1 protein in both size and expression levels. The apparent molecular mass of the NHE1 protein was approximately 100 kDa, which is not consistent with removal of these two transmembrane segments. Additionally, the introduction of cysteine residues in this region produced proteins that were accessible to extracellular labeling. For example T97 and T101 were both accessible to extracellular MTSET, which indicated that these amino acids were present in the full-length intact protein. Further, this confirms an extracellular localization for extracellular loop 1 which is comprised of amino acid residues 35 to 104. Our results with amino acid residues T97 and T101 confirm that this more proximal region is also accessible from the extracellular surface. Amino acid residue S44 was not readily accessible in our experiments in contrast to the earlier report [19]. The reason for this is not clear but this does not detract from the preponderance of evidence which shows that this region of the protein is extracellular, and a part of the intact full length NHE1 protein.

The amino acid residue at position number 8 was returned to its native Cys from a Ser residue in the cNHE1 protein. It was not accessible to extracellular MTSET. However, when cells were permeabilized with streptolysin O, this amino acid became accessible. This confirmed that this short N-terminal extension of NHE1 was present in the full length protein and supports and intracellular localization, consistent with the model #1 [19].

The above data suggest that amino acid residues 1–101 are present in the full-length protein. However, an argument could be made that this was only a fraction of the NHE1 protein that we examined and that the first two segments are removed from most of the NHE1 protein that is present on the cell surface. While this seems unlikely, we provided evidence against it and further evidence that amino acids 40–105 form an extracellular loop present in the intact full-length protein. Counillon et al. [40] showed that only consensus site for N-linked glycosylation of NHE1 is on N75. Our experiments were to demonstrate that this site on the protein was present at the cell surface. To do this, we used protein with or without this site that had been recovered from the cell surface by cell surface labeling the proteins with biotin and recovering them with streptavidin. Thus any NHE1 protein could not have been from within the cell. We found that protein containing the N75 site was present on the cell surface. Mutation of amino acid N75 showed that the glycosylation was at this location even though both

the glycosylated and un-glycosylated protein were both targeted to the cell surface (Fig. 4B,C). These results confirm that the NHE1 protein on the cell surface contained the N75 site. We also found that the enzyme PNGaseF reduced the molecular weight of the NHE1 that was recovered from the cell surface as described above. This further confirmed that the extracellular NHE1 was glycosylated (Fig. 4A). Of note also, the apparent molecular weight of the protein from the cell surface that was either deglycosylated enzymatically, or had the N75D mutation, was approximately 100 kDa. Removal of the first two transmembrane segments would result in a protein of approximately 81.5 kDa with the HA tag. This also suggests that the first 127 amino acid residues remain on the plasma membrane NHE1 protein. Taken together, the experiments demonstrate that the N75 site is present on the mature NHE1 protein on the cell surface, confirming that this region is present in the mature protein.

The next set of experiments was to examine the transmembrane segment containing amino acid residues 315–411. Thirteen mutations were made in this general region. Fig. 5 shows schematic diagrams of the two alternate models of amino acid residues 315–411. Results of our experiments are shown with solid colors, red indicating a residue inaccessible from the extracellular surface, and green indicating a residue accessible from the extracellular surface. Results from the study of Wakabayashi et al. [19] are also indicated with cross hatches using the same color scheme. We made six mutations between amino acids 315 and 345. All of these were not accessible from the exterior of the cell including amino acid position 326 (Figs. 5, 3B). The results with residues 318 and 320 are consistent with either model (Fig. 5). Results with residues 326 are also consistent with either model. Though it was previously demonstrated that residues 324 and 325 are accessible from the outside (Fig. 5) it was hypothesized [19] that this was due to an infolding of this intracellular loop. When cells were permeabilized with streptolysin O, residues at position 318, 320, 326, and 338 became accessible. This further supports an intracellular location for these residues. Streptolysin O has been used earlier to permeabilize cells and determine if particular amino acids of transmembrane proteins have an intracellular location. However, it would not result in accessibility within the plane of the membrane, which allows an assignment to intracellular loops between transmembrane domains [19,41].

Amino acid residues 344 and 345 were not accessible from outside the cell. This was more consistent with model 1 and inconsistent with the model #2 [20] which placed them on an extracellular side of the membrane. Permeabilization of the cells with streptolysin O rendered residue 345 accessible, further supporting an intracellular location, and again supporting model #1.

The segment from amino acid residue 363 to residue 381 is proposed to be an extracellular loop in model #1 but is proposed to be intracellular in model #2 [20]. We made 4 mutant proteins in this region that we characterized. Three of these (with mutations at 306, 369 and 377) were readily accessible from the extracellular surface. Amino acid residue at position 371 was not. Previous experiments showed that 8 other amino acid residues within this segment (Fig. 5) are also accessible from the extracellular face. Overall, this gives a very strong preponderance of evidence favoring this segment as an extracellular loop and not being intracellular or embedded within the membrane. Though one amino acid residue (371) was inaccessible from outside the cell, this can easily be explained as being due to folding of the extracellular loop which might prevent extracellular chemical association, something we have seen earlier [16].

Accessibility studies of amino acid residues 401–411 also place this region on the outside of the cell. Our studies placed residues 401 and 402 outside the cell, which agrees with earlier studies that confirmed that amino acids 407–409 are outside the cell. While we did find that amino acid position 406 was not accessible, the large preponderance of evidence is that this region is extracellular, which is in agreement with both models.

4.3. Conclusion

Overall, our study on the region from amino acid residue 315 to residue 411 supports model #1 proposed by Wakabayashi [19] and Nygaard et al. [21] and disagrees with the model proposed by Landau [20]. The evidence of our own study, summarized, is that residues between the segment 315 and 345 are not accessible from the exterior of the cell, and that the residues 363–381 are accessible from the exterior of the cell. These two observations are inconsistent with placing these two regions on the opposite side of the membrane as proposed in model #2 [20]. Additionally, our evidence is in agreement with the cysteine scanning accessibility experiments reported earlier [19] and with the modeling reported by Nygaard et al. [42] which makes a sum total of a large number of experiments from three laboratories, that

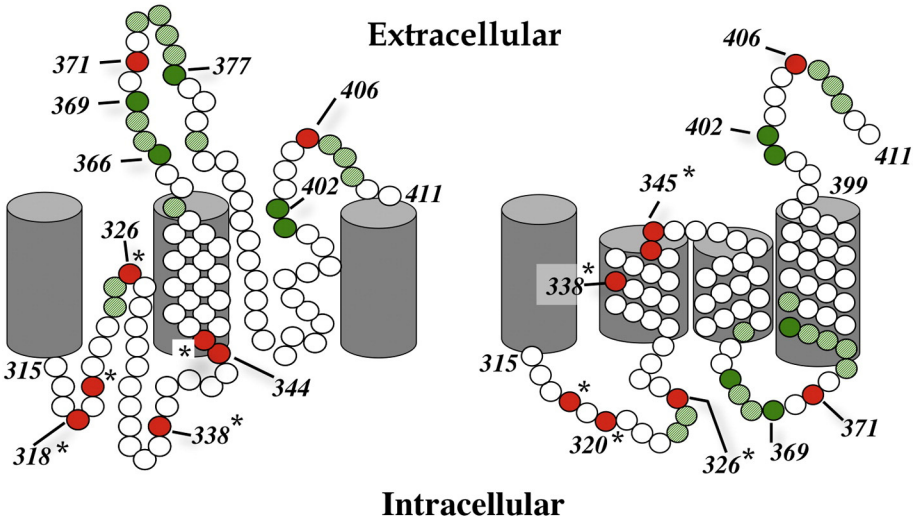

Fig. 5. Alternate topology models of amino acid residues 315–411 of the NHE1 protein. Left panel, topology after Wakabayashi et al. [19]. Right panel model after Landau et al. [20]. Green filled residue indicates results from the present study indicating residues accessible to MTSET blockage of reactivity with IRDye800-maleimide in intact cells (indicating extracellular accessibility). Red filled residue indicates results from the present study indicating residues not accessible to MTSET blockage of reactivity with IRDye800-maleimide in intact cells (indicating lack of accessibility). Results from Wakabayashi et al. [19] are also illustrated for comparative purposes, green stripes indicate extracellular accessibility, red stripes indicate lack of extracellular accessibility. *Indicates the residue became accessible after cells were permeabilized with streptolysin O. (For interpretation of the references to color in this figure legend, the reader is referred to the web version of this article.)

place residues 315 to residue 345 in an intracellular location and residues 363–381 outside of the cell.

We suggest that model #1 [19,21] is correct or much more representative of the true structure of NHE1 for both the presence of the first two transmembrane segments on the protein, and for its proposed topology of amino acid residues 315–411.

Conflict of interest

No conflicts of interest to declare.

Transparency document

The Transparency document associated with this article can be found, in the online version.

Acknowledgments

This work was supported by funding from CIHR #MOP-114876 to LF.

References

[1] C. Sardet, A. Franchi, J. Pouysségur, Molecular cloning, primary structure, and expression of the human growth factor-activatable Na^+/H^+ antiporter, Cell 56 (1989) 271–280.
[2] L. Fliegel, Molecular biology of the myocardial Na^+/H^+ exchanger, J. Mol. Cell. Cardiol. 44 (2008) 228–237.
[3] B.L. Lee, B.D. Sykes, L. Fliegel, Structural and functional insights into the cardiac Na(+)/H(+) exchanger, J. Mol. Cell. Cardiol. 61 (2013) 60–67.
[4] S.J. Reshkin, A. Bellizzi, S. Caldeira, V. Albarani, I. Malanchi, M. Poignee, M. Alunni-Fabbroni, V. Casavola, M. Tommasino, Na^+/H^+ exchanger-dependent intracellular alkalinization is an early event in malignant transformation and plays an essential role in the development of subsequent transformation-associated phenotypes, FASEB J. 14 (2000) 2185–2197.
[5] S.R. Amith, L. Fliegel, Regulation of the Na^+/H^+ exchanger (NHE1) in breast cancer metastasis, Cancer Res. 73 (2013) 1259–1264.
[6] G.A. Cox, C.M. Lutz, C.-L. Yang, D. Biemesderfer, R.T. Bronson, A. Fu, P.S. Aronson, J.L. Noebels, W.N. Frankel, Sodium/hydrogen exchanger gene defect in slow-wave epilepsy mice, Cell 91 (1997) 139–148.
[7] C. Guissart, X. Li, B. Leheup, N. Drouot, B. Montaut-Verient, E. Raffo, P. Jonveaux, A.F. Roux, M. Claustres, L. Fliegel, M. Koenig, Mutation of SLC9A1, encoding the major Na^+/H^+ exchanger, causes ataxia-deafness Lichtenstein–Knorr syndrome, Hum. Mol. Genet. 24 (2015) 463–470.
[8] C. Hunte, E. Screpanti, M. Venturi, A. Rimon, E. Padan, H. Michel, Structure of a Na^+/H^+ antiporter and insights into mechanism of action and regulation by pH, Nature 435 (2005) 1197–1202.
[9] C. Lee, H.J. Kang, C. von Ballmoos, S. Newstead, P. Uzdavinys, D.L. Dotson, S. Iwata, O. Beckstein, A.D. Cameron, D. Drew, A two-domain elevator mechanism for sodium/proton antiport, Nature 501 (2013) 573–577.
[10] C. Paulino, W. Kuhlbrandt, pH- and sodium-induced changes in a sodium/proton antiporter, Elife 3 (2014) e01412.
[11] P. Goswami, C. Paulino, D. Hizlan, J. Vonck, O. Yildiz, W. Kuhlbrandt, Structure of the archaeal Na^+/H^+ antiporter NhaP1 and functional role of transmembrane helix 1, EMBO J. 30 (2011) 439–449.
[12] C. Alves, B.L. Lee, B.D. Sykes, L. Fliegel, Structural and functional analysis of the transmembrane segment pair VI and VII of the NHE1 isoform of the Na^+/H^+ exchanger, Biochemistry 53 (2014) 3658–3670.
[13] B.L. Lee, Y. Liu, X. Li, B.D. Sykes, L. Fliegel, Structural and functional analysis of extracellular loop 4 of the Nhe1 isoform of the Na(+)/H(+) exchanger, Biochim. Biophys. Acta 1818 (2012) 2783–2790.
[14] J. Tzeng, B.L. Lee, B.D. Sykes, L. Fliegel, Structural and functional analysis of critical amino acids in TMVI of the NHE1 isoform of the Na^+/H^+ exchanger, Biochim. Biophys. Acta 1808 (2011) 2327–2335.
[15] J. Tzeng, B.L. Lee, B.D. Sykes, L. Fliegel, Structural and functional analysis of transmembrane segment VI of the NHE1 isoform of the Na^+/H^+ exchanger, J. Biol. Chem. 285 (2010) 36656–36665.
[16] B.L. Lee, X. Li, Y. Liu, B.D. Sykes, L. Fliegel, Structural and functional analysis of extracellular loop 2 of the Na(+)/H(+) exchanger, Biochim. Biophys. Acta 1788 (2009) 2481–2488.
[17] T. Reddy, J. Ding, X. Li, B.D. Sykes, J.K. Rainey, L. Fliegel, Structural and functional characterization of transmembrane segment IX of the NHE1 isoform of the Na^+/H^+ exchanger, J. Biol. Chem. 283 (2008) 22018–22030.
[18] E.R. Slepkov, J.K. Rainey, X. Li, Y. Liu, F.J. Cheng, D.A. Lindhout, B.D. Sykes, L. Fliegel, Structural and functional characterization of transmembrane segment IV of the NHE1 isoform of the Na^+/H^+ exchanger, J. Biol. Chem. 280 (2005) 17863–17872.
[19] S. Wakabayashi, T. Pang, X. Su, M. Shigekawa, A novel topology model of the human Na^+/H^+ exchanger isoform 1, J. Biol. Chem. 275 (2000) 7942–7949.
[20] M. Landau, K. Herz, E. Padan, N. Ben-Tal, Model structure of the Na^+/H^+ exchanger 1 (NHE1): functional and clinical implications, J. Biol. Chem. 282 (2007) 37854–37863.
[21] E.B. Nygaard, J.O. Lagerstedt, G. Bjerre, B. Shi, M. Budamagunta, K.A. Poulsen, S. Meinild, R.R. Rigor, J.C. Voss, P.M. Cala, S.F. Pedersen, Structural modeling and electron paramagnetic resonance spectroscopy of the human Na^+/H^+ exchanger isoform 1, NHE1, J. Biol. Chem. 286 (2011) 634–648.
[22] R. Hendus-Altenburger, B.B. Kragelund, S.F. Pedersen, Structural dynamics and regulation of the mammalian SLC9A family of Na(+)/H(+) exchangers, Curr. Top. Membr. 73 (2014) 69–148.
[23] E. Slepkov, J. Ding, J. Han, L. Fliegel, Mutational analysis of potential pore-lining amino acids in TM IV of the Na(+)/H(+) exchanger, Biochim. Biophys. Acta 1768 (2007) 2882–2889.
[24] M. Schushan, M. Landau, E. Padan, N. Ben-Tal, Two conflicting NHE1 model structures: compatibility with experimental data and implications for the transport mechanism, J. Biol. Chem. 286 (2011) le9 (author reply le10).
[25] P.M. Cala, S.F. Pedersen, Response to Schushan, et al., Two conflicting NHE1 model structures: compatibility with experimental data and implications for the transport mechanism, J. Biol. Chem. 286 (2011) le10, http://dx.doi.org/10.1074/jbc.N1110.159202.
[26] X. Li, J. Ding, Y. Liu, B.J. Brix, L. Fliegel, Functional analysis of acidic amino acids in the cytosolic tail of the Na^+/H^+ exchanger, Biochemistry 43 (2004) 16477–16486.
[27] E.R. Slepkov, S. Chow, M.J. Lemieux, L. Fliegel, Proline residues in transmembrane segment IV are critical for activity, expression and targeting of the Na^+/H^+ exchanger isoform 1, Biochem. J. 379 (2004) 31–38.
[28] M. Michalak, L. Fliegel, K. Wlasichuk, Isolation and characterization of calcium binding glycoproteins of cardiac sarcolemmal vesicles, J. Biol. Chem. 265 (1990) 5869–5874.
[29] B.L. Lee, X. Li, Y. Liu, B.D. Sykes, L. Fliegel, Structural and functional analysis of transmembrane XI of the NHE1 isoform of the Na^+/H^+ exchanger, J. Biol. Chem. 284 (2009) 11546–11556.
[30] K. Moncoq, G. Kemp, X. Li, L. Fliegel, H.S. Young, Dimeric structure of human Na^+/H^+ exchanger isoform 1 overproduced in *Saccharomyces cerevisiae*, J. Biol. Chem. 283 (2008) 4145–4154.
[31] L. Counillon, J. Pouysségur, R.A.F. Reithmeier, The Na^+/H^+ exchanger NHE-1 possesses N- and O-linked glycosylation restricted to the first N-terminal extracellular domain, Biochemie 33 (1994) 10463–10469.
[32] L. Fliegel, Regulation of the Na^+/H^+ exchanger in the healthy and diseased myocardium, Expert Opin. Ther. Targets 13 (2009) 55–68.
[33] M. Karmazyn, A. Kilic, S. Javadov, The role of NHE-1 in myocardial hypertrophy and remodelling, J. Mol. Cell. Cardiol. 44 (2008) 647–653.
[34] A. Odunewu-Aderibigbe, L. Fliegel, The Na(+)/H(+) exchanger and pH regulation in the heart, IUBMB Life 66 (2014) 679–685.
[35] H. Liu, P.M. Cala, S.E. Anderson, Ethylisopropylamiloride diminishes changes in intracellular Na, Ca and pH in ischemic newborn myocardium, J. Mol. Cell. Cardiol. 29 (1997) 2077–2086.
[36] M. Karmazyn, NHE-1: still a viable therapeutic target, J. Mol. Cell. Cardiol. 61 (2013) 77–82.
[37] B. Masereel, L. Pochet, D. Laeckmann, An overview of inhibitors of Na(+)/H(+) exchanger, Eur. J. Med. Chem. 38 (2003) 547–554.
[38] C. Harris, L. Fliegel, Amiloride and the Na^+/H^+ exchanger protein. Mechanism and significance of inhibition of the Na^+/H^+ exchanger, Int. J. Mol. Med. 3 (1999) 315–321.
[39] S.F. Pedersen, S.A. King, E.B. Nygaard, R.R. Rigor, P.M. Cala, NHE1 inhibition by amiloride- and benzoylguanidine-type compounds. Inhibitor binding loci deduced from chimeras of NHE1 homologues with endogenous differences in inhibitor sensitivity, J. Biol. Chem. 282 (2007) 19716–19727.
[40] L. Counillon, J. Pouyssegur, R.A. Reithmeier, The Na^+/H^+ exchanger NHE-1 possesses N- and O-linked glycosylation restricted to the first N-terminal extracellular domain, Biochemistry 33 (1994) 10463–10469.
[41] W. Cao, L.H. Matherly, Analysis of the membrane topology for transmembrane domains 7–12 of the human reduced folate carrier by scanning cysteine accessibility methods, Biochem. J. 378 (2004) 201–206.
[42] H. Liu, P.M. Cala, S.E. Anderson, Ischemic preconditioning: effects on pH, Na and Ca in newborn rabbit hearts during ischemia/reperfusion, J. Mol. Cell. Cardiol. 30 (1998) 685–697.